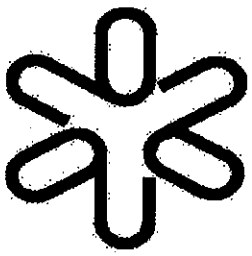

Instituto de Física
Universidade de São Paulo

ELASTIC-TRANSFER: A NON-DISPERSIVE COMPONENT IN THE OPTICAL POTENTIAL, AND ITS EFFECT ON THE $^{12}C+^{24}Mg$ ELASTIC SCATTERING

LÉPINE-SZILY, A.; HUSSEIN, M. S.;
LICHTENTHÄLER,R.; CSEH, J.; LÉVAI, G.
DEPTO. FÍSICA NUCLEAR

Publicação IF - 1330/98

UNIVERSIDADE DE SÃO PAULO
Instituto de Física
Cidade Universitária
Caixa Postal 66.318
05315-970 - São Paulo - Brasil

DEPARTAMENTO DE FÍSICA NUCLEAR
INSTITUTO DE FÍSICA
UNIVERSIDADE DE SÃO PAULO

IFUSP - DFN/98-006

Elastic-Transfer: a Non-Dispersive Component in the Optical Potential, and its Effect on the $^{12}C+^{24}Mg$ Elastic Scattering

A. Lépine-Szily
M.S. Hussein
R. Lichtenthäler
J. Cseh
G. Lévai

Dedicated to Prof. A.F.R. de Toledo Piza on the occasion of his 60th birthday

Elastic-transfer: a non-dispersive component in the optical potential, and its effect on the $^{12}C+^{24}Mg$ elastic scattering *

A. Lépine-Szily[1], M. S. Hussein[1], R. Lichtenthäler[1], J. Cseh[2], G, Lévai[2]
1. IFUSP-Universidade de São Paulo, C.P.66318, 05315-970 São Paulo, Brasil
2. MTA ATOMKI, Debrecen Pf.51, Hungary-4001

November 27, 1998

Abstract

It is emphasized that the coupling of the elastic channel to an elastic transfer channel leads to a non-dispersive polarization potential with a periodic energy dependence. Evidence of this is found in the elastic scattering data of $^{12}C+^{24}Mg$ at low energies. The finding hints at a significant $^{12}C+^{12}C$ clustering effect in the ground state of ^{24}Mg.

The dispersive optical potential usually referred to as the Feshbach potential [1], obeys a dispersion relation. In the heavy ion context this relation has gained notoriety in recent years and is usually referred to as the Threshold Anomaly (TA). As eloquently explained by Satchler [2], the dispersion relation of the Feshbach potential comes about as a consequence of the polarization nature in the sense that the potential has the general structure:

$$V_{Feshbach}(r,r') = \sum_{i=1}^{n} V_{oi}(r) < r \mid \frac{1}{E - H_i + i\epsilon} \mid r' > V_{io}(r') \tag{1}$$

The intermediate channel Green operator, $(E-H_i+i\epsilon)^{-1}$, has the following simple structure:

$$(E - H_i + i\epsilon)^{-1} = -i\pi\delta(E - H_i) + P\frac{1}{E - H_i} \tag{2}$$

where P stands for the principal part and H_i is taken for simplicity to be Hermitian. Clearly, one can write:

$$P\frac{1}{E - H_i} = P\int dz \frac{\delta(z - H_i)}{E - z} = -\frac{P}{\pi}\int dz \frac{-\pi\delta(z - H_i)}{E - z} \tag{3}$$

*Dedicated to Prof. A. F. R. Toledo Piza on the occasion of his 60th birthday.

From equations 1 and 3 one finds the dispersion relation:

$$ReV_{Feshbach}(r, r', E) = \frac{P}{\pi} \int dz \frac{Im V_{Feshbach}(z, r, r')}{z - E}, \tag{4}$$

which can be generalized to the whole $V_{Feshbach}$ Eq. (1). The generalization of the dispersion relation for the case of non-hermitian H_i is given in Ref. [3]. This reference shows that Eq. (4) still holds. In actual use in data analysis one relies on local potentials. The intrinsically non-local dispersive Feshbach potential is therefore transformed into a local-equivalent one. This brings in more subtle energy dependence. We should point out that the non-dispersive "bare" part of the intercation is also non-local owing to the Pauli exchange effects. In its local equivalent version the bare interaction also carries important energy dependence as has been stressed recently in [4-6]. In practical application, it was found [7] that the local-equivalent Feshbach potential potential at a given value of the now one spatial variable r, still satisfies Eq. (4)

Now we raise the following question: do all channel couplings result in a dispersive Feshbach potential? The answer is no, at least in cases involving elastic transfer. Here we mean a process which involves the elastic scattering of the following objects.

$$(a + b) + b \longrightarrow (a + b) + b \tag{5}$$

$$(a + b) + b \longrightarrow b + (a + b) \tag{6}$$

The two corresponding amplitudes add coherently. Since the projectile – target system, in the second process, becomes the target – projectile system (no change in internal structure) the second process in Eq. (6), the elastic transfer process, is important at large angles. The Feshbach potential that takes into account the coupling of the elastic channel to the elastic transfer channel is found to be [8,9]

$$V_{Feshbach}^{elastic-transfer} = (-1)^l F(r) \tag{7}$$

where l is the orbital angular momentum and $F(r)$ is an approximate transfer form-factor of the second process in Eq. (6). There is no energy dependence in (7). Clearly, (7) does not satisfy any energy dispersion relation. Of course some weak energy dependence may be found in $V_{Feshbach}^{elastic-transfer}$, when higher-order processes are taken into account, e.g.:

$$(a + b) + b \longrightarrow (a + b)^* + b \longrightarrow b + (a + b) \tag{8}$$

In the following we ignore these processes for simplicity. The above discussion may become very important in situations where elastic transfer is significant. Such a situation may occur not only in nuclear but also in atom-atom scattering.

In a recent experiment [10,11] the complete angular distributions of the elastic scattering of $^{12}C+^{24}Mg$ were measured at fifteen energies near the Coulomb barrier, namely between E_{cm} = 10.67 and 16.00 MeV. The data were analysed in the optical model framework (Pot II) and the best-fit potentials were: shallow, energy dependent, real potentials (V_o $\sim$ 37 MeV, r_o=1.29 fm, a=0.4 fm) with no continuous ambiguity and very weak, energy dependent, imaginary potentials ($W_o/V_o \sim 0.01$, W_o=0.5–1.5 MeV, r_i=1.77 fm, $a_i \sim$ 0.4–0.8 fm).

We present in figure 1a some of the lowest energy angular distributions, situated at energies under and at the Coulomb barrier (V_{CB}=12.67 MeV using the Christensen–Winther radius) together with the optical model fits. The angular distributions present clear oscillatory pattern even at the lowest energies. In figure 1b the low-energy elastic scattering angular distributions of $^{12}C+^{28}Si$ system are presented. These unpublished data [12] were also measured at the Pelletron Laboratory of the São Paulo University, and will be published in the near future together with an optical model analysis. The optical model used to reproduce the data is much more absorptive (3 to 5 times more), then the Pot. II used for the $^{12}C+^{24}Mg$ system. The Christensen–Winther Coulomb barrier for the $^{12}C+^{28}Si$ system is V_{CB}=14.36 MeV. We indicate in the figure caption the ratio E_{cm}/V_{CB} to allow a quantitative comparison between angular distributions of figure 1a and 1b.

It is clear that the angular distributions at the same energy with respect to the Coulomb barrier are different for the two systems considered. While the oscillations are clear for the $^{12}C+^{24}Mg$ system, even at energies under the Coulomb barrier, they are smooth and non-oscillating for the $^{12}C+^{28}Si$ system at the same energies. Even at energies 12% above the Coulomb barrier, where the very back angle region of the $^{12}C+^{28}Si$ begins to show one oscillation, the $^{12}C+^{28}Mg$ system shows much more oscillations in the intermediate angle region.

Both optical potentials are dependent on the bombarding energy. From the point of view of radial dependences, their differences can be pinned down in the notch-test. This test consists in summing a localized perturbation to the optical potential at variable radial positions and observe the quality of the fit (defined through the χ^2) as a function of the position of the perturbation. It showed very different results for the two systems. For the $^{12}C+^{28}Si$ system the notch test presents a localized peak at R_1+R_2=7.3 fm, which means that the elastic data are sensitive to the optical potential only in a radially restricted region at the nuclear surface around 7.3 fm. For the $^{12}C+^{24}Mg$ system the notch test indicates that the elastic data are sensitive to the optical potential on the surface and in the nuclear interior, from 3 to 8 fm, result compatible with the very transparent optical potentials used to fit the data [11].

The differences between the two potentials become even more interesting, when they are compared from the point of view of their energy dependences, through the dispersion relation (Eq. 4). While the optical potentials of the $^{12}C+^{28}Si$ system satisfy the dispersion

relation at the R=7.3 fm, the optical potentials of the ^{12}C+^{24}Mg system do not satisfy the dispersion relation at any radius (see Fig.2). Nevertheless the volume integrals of the optical potentials of the ^{12}C+^{24}Mg system satisfy the dispersion relation as it was shown previously [10,11].

We can calculate the differences between the real part of the optical potential and the real part of the dispersive potential, also called Feshbach potential in the introductory discussion. The real part of the Feshbach potential is calculated from the imaginary optical potential through the dispersion relation. The plot of these differences as a function of the energy is presented in Figure 3.

In the case of the ^{12}C+^{28}Si system, at least at these very low energies, the difference called $ReV_{non-dispersive}$ is zero, while for the ^{12}C+^{24}Mg system it presents a clearly oscillatory pattern, as a function of energy, with a decreasing amplitude, when the radius increases. If we assume that the non-dispersive part of the potential is responsible for the coupling of the elastic channel to the elastic transfer channel, then from the point of view of Eqs. (4) and (7), we can write:

$$ReV_{opt.mod} - ReV_{Feshbach} = ReV_{non-dispersive} = (-1)^l F(r) = cos(\pi l(r,E))F(r), \qquad (9)$$

where a semiclassical interpretation was invoked to transform the l-dependence into an r- and E-dependences. Here $l(r,E)$ is a function to be obtained from the classical turning point condition:

$$E = V(r) + \frac{\hbar^2 l(l+1)}{2\mu r^2} \qquad (10)$$

Then qualitatively the non-dispersive part of the potential should have an oscillatory character ($\cos\pi l$) and decrease in ampitude with increasing r ($F(r)$), as it appears in Fig. 3. We also show in Fig. 3 a very qualitative fit to $ReV_{non-dispersive}$, by a cosine function. We assumed that the argument of the cosine function, which is $\pi\tilde{l}$, where $\tilde{l}$ is an orbital angular momentum like quantity, which varies as $\sqrt{E}$ and linearly with r. The argument for the cosine function in the three fits was roughly :

$$\pi\tilde{l} = Const \times \sqrt{E} \times r \qquad (11)$$

This is different from that obtained from the classical turning point relation:
$l = Const\sqrt{1-\frac{V}{E}}\sqrt{E}r$.

The reaction amplitudes of Eqs. (5) and (6) can interfere only in case the cluster b is present in the target. Thus, from the nuclear structure point of view the crucial question is whether or not the (exotic) cluster corresponding to the projectile nucleus is present in the ground state of the target.

In light nuclei, the $U(3)$ symmetry is known to be approximately valid [13], therefore, these kind of questions can be investigated by applying a $U(3)$ selection rule. The problem

is relatively simple due to the fact that the nuclear states can be characterized by a single irreducible representation (irrep) of the $U(3)$ group, called leading irrep. The selection rule requires a matching between the $U(3)$ representation of the parent nucleus, described by the $[n_1, n_2, n_3]$ Young pattern, and one of the representations, obtained from coupling those of the daughter nuclei ($[n_1^{c_i}, n_2^{c_i}, n_3^{c_i}]$, $i = 1, 2$), with the relative motion ($[n, 0, 0]$):

$$[n_1^{c_1}, n_2^{c_1}, n_3^{c_1}] \otimes [n_1^{c_2}, n_2^{c_2}, n_3^{c_2}] \otimes [n, 0, 0] = \sum_k \oplus [n_{1,k}^c, n_{2,k}^c, n_{3,k}^c]. \quad (12)$$

Here $\otimes$ means direct product, and $\oplus$ indicates direct sum. The number of the relative motion quanta is fixed by the Wildermuth condition [14], i.e. by the requirement that the total number of quanta of the whole system (clusters and relative motion) have to be greater or equal than the lowest possible number of oscillation quanta allowed by Pauli's Principle in the parent nucleus. For details, see Ref. [15]. This selection rule is based on the equivalence of the Hamiltonians of the shell model and the cluster model. For harmonic oscillator approximation it was shown to be valid in the early days of cluster studies, [14], but it turns out to be valid for more realistic interactions as well [16].

For different samples of light nuclei this selection rule has been applied systematically [17,18]. As a result we have found that (in the leading term approximation) the ^{12}C cluster is present in the ground state of the ^{24}Mg nucleus, but is absent from the ground state of the ^{28}Si. (For these two nuclei more detailed cluster calculation have also been carried out in the algebraic framework, which incorporated a large number of excited states, as well [19,20].)

The different oscillatory pattern of Figs. 1a and 1b, as well as the different nature of the corresponding potentials, as discussed in the previous sections, seem to justify the predictions of the nuclear cluster model. Actually, the coherence effect between the reaction amplitudes of Eq. (5) and (6) can be considered as the fingerprint of the exotic (projectile-like) clusterization in the ground state of the target nucleus. It can be considered as a promising and effective way of hunting for the clusterization in the ground states of light nuclei, which is a very difficult task otherwise.

In conclusion, experimental evidence has been presented in this paper in favor of a non-dispersive component in the Feshbach potential, which is traced to the coupling of the elastic channel to an elastic transfer channel. The system ^{12}C+^{24}Mg was used for the purpose. The finding may shed light on cluster effect in the ground state of light nuclei.

1. H. Feshbach, Theoretical Nuclear Physics II, Nuclear Reactions, Wiley.
2. G. R. Satchler, Phys. Rep.**199**, 147 (1991)
3. B. V. Carlsson, T. Frederico, M. S. Hussein, H. Esbensen and S. Landowne, Phys. Rev. **C41**, 933 (1990).

4. M. A. Cândido Ribeiro, L. C. Chamon, D. Pereira, M. S. Hussein and D. Galetti, Phys. Rev. Lett. **78**,3270 (1997).
5. L. C. Chamon, D. Pereira, M. S. Hussein, M. A. Cândido Ribeiro and D. Galetti, Phys. Rev. Lett. **79**, 5218 (1997).
6. L. C. Chamon, D. Pereria and M. S. Hussein, Phys. Rev. **C 58**,576 (1998).
7. C. Mahaux, H. Ngô, G. R. Satchler, Nucl. Phys. **A 449**,354 (1986).
8. W. E. Frahn, Diffractive Processes in Nuclear Physics, Oxford University Press.
9. W. von Oertzen and H. G. Bohlen, Phys. Rep. **19**,1 (1975).
10. A. Lépine–Szily, W. Sciani, Y. K. Watari, W. Mittig, R. Lichtenthaler, M. M. Obuti, J. M. Oliveira Jr., A. C. C. Villari, Phys. Lett. **B 304**,45 (1993).
11. W. Sciani, A. Lépine–Szily, R. Lichtenthaler, P. Fachini, L.C. Gomes, G. F. Lima, M. M. Obuti, J. M. Oliveira Jr., A. C. C. Villari, Nucl. Phys. **A 620**,91 (1997).
12. J. M. Oliveira Jr. Thesis, unpublished, IFUSP.
13. J. P. Elliott, Proc. Roy. Soc. **A245** 128 and 562 (1958).
14. K. Wildermuth, Th. Kanellopoulos, Nucl. Phys. **7** 150 (1958); K. Wildermuth, Y. C. Tang, A unified theory of the nucleus (Academic Press, New York, 1977).
15. J. Cseh, G. Lévai, Ann. Phys. (NY) **230** 165 (1994).
16. J. Cseh, Heavy Ion Physics **7** 23 (1998).
17. J. Cseh and W. Scheid, J. Phys. **G18**, 1419 (1992).
18. J. Cseh, J. Phys. **G19**, L97 (1993).
19. J. Cseh, G. Lévai, W. Scheid, Phys. Rev. **C 48** (1993) 1724.
20. J. Cseh, Phys. Rev. **C50**, 2240 (1994);

Figure Captions

Figure 1a. The $^{12}C+^{24}Mg$ elastic scattering angular distributions, measured at the indicated energies, are represented by the dots. The solid lines are optical model calculations with our best fit optical potentials (Pot. II). The E_{CM}/V_{CB} values at these energies are respectively, 0.947, 1.026 and 1.105, with V_{CB}=12.67 MeV.

Figure 1b. The $^{12}C+^{28}Si$ elastic scattering angular distributions, measured at the indicated energies, are represented by the dots. The solid lines are optical model calculations with our best fit optical potentials. The E_{CM}/V_{CB} values at these energies are respectively, 0.926, 1.023, 1.120 with V_{CB}=14.36 MeV.

Figure 2. The imaginary and the real depths of the best fit optical potentials of the $^{12}C+^{24}Mg$ system, as a function of the laboratory energies (squares) for R=7.1 fm. We also used data at higher energies (E_{lab}=37.9 and 40.0 MeV [10,11]) to fix the imaginary part of the potential. The dispersion relation calculations are indicated by dots and the disagreement with the real optical potential is evident.

Figure 3. The differences between the real part of the optical potential and the real part of the dispersive potential (calculated by the dispersion relation) as a function of the laboratory energy, at three radial positions, R=5.5 fm, 6.5 fm and 7.1 fm. Discussion of the solid line in text.

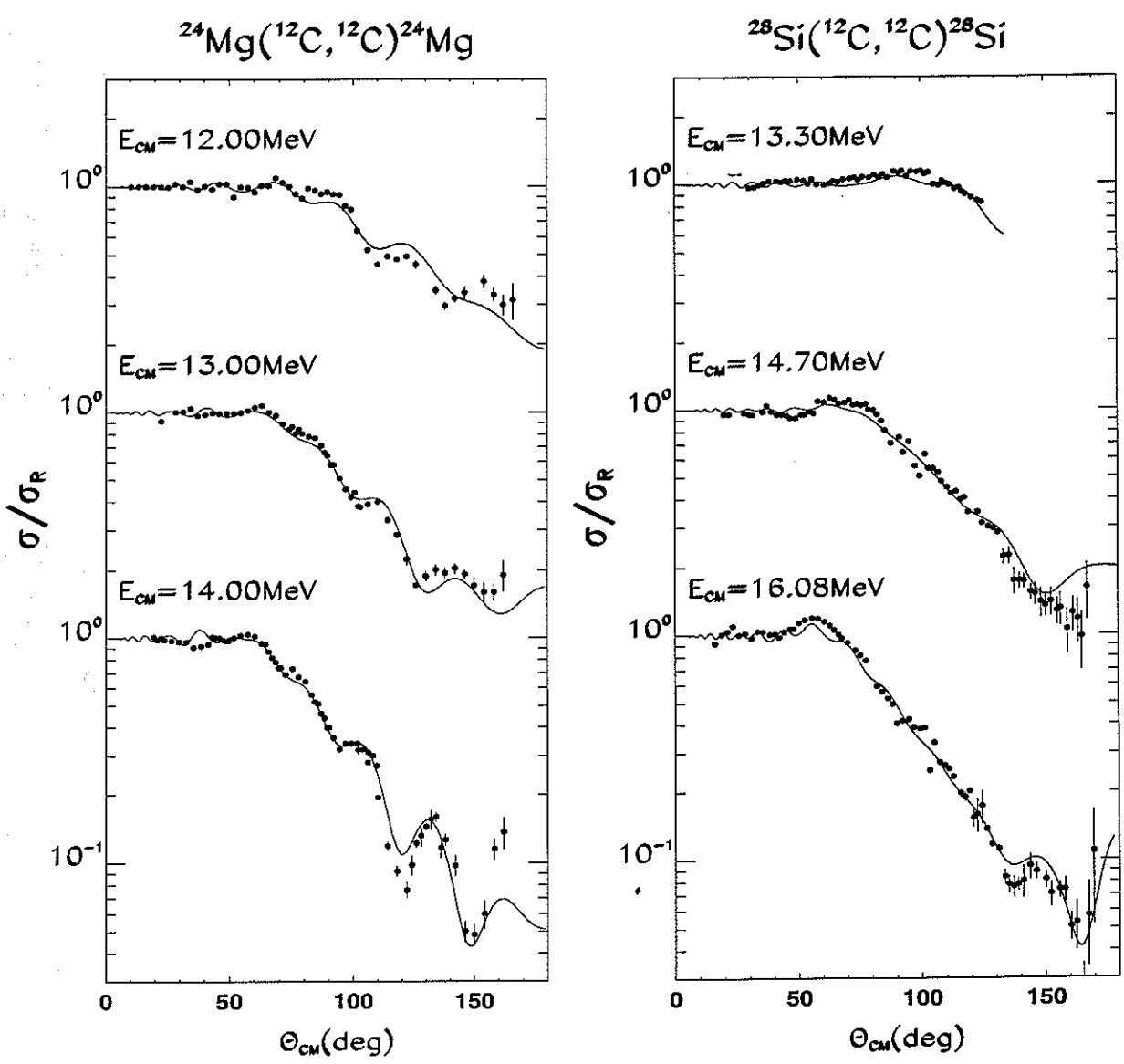
$^{24}Mg(^{12}C,^{12}C)^{24}Mg$
$^{28}Si(^{12}C,^{12}C)^{28}Si$
E_{CM}=12.00MeV
E_{CM}=13.00MeV
E_{CM}=14.00MeV
E_{CM}=13.30MeV
E_{CM}=14.70MeV
E_{CM}=16.08MeV
σ/σ_R
10^0
10^{-1}
0
50
100
150
Θ_{CM}(deg)

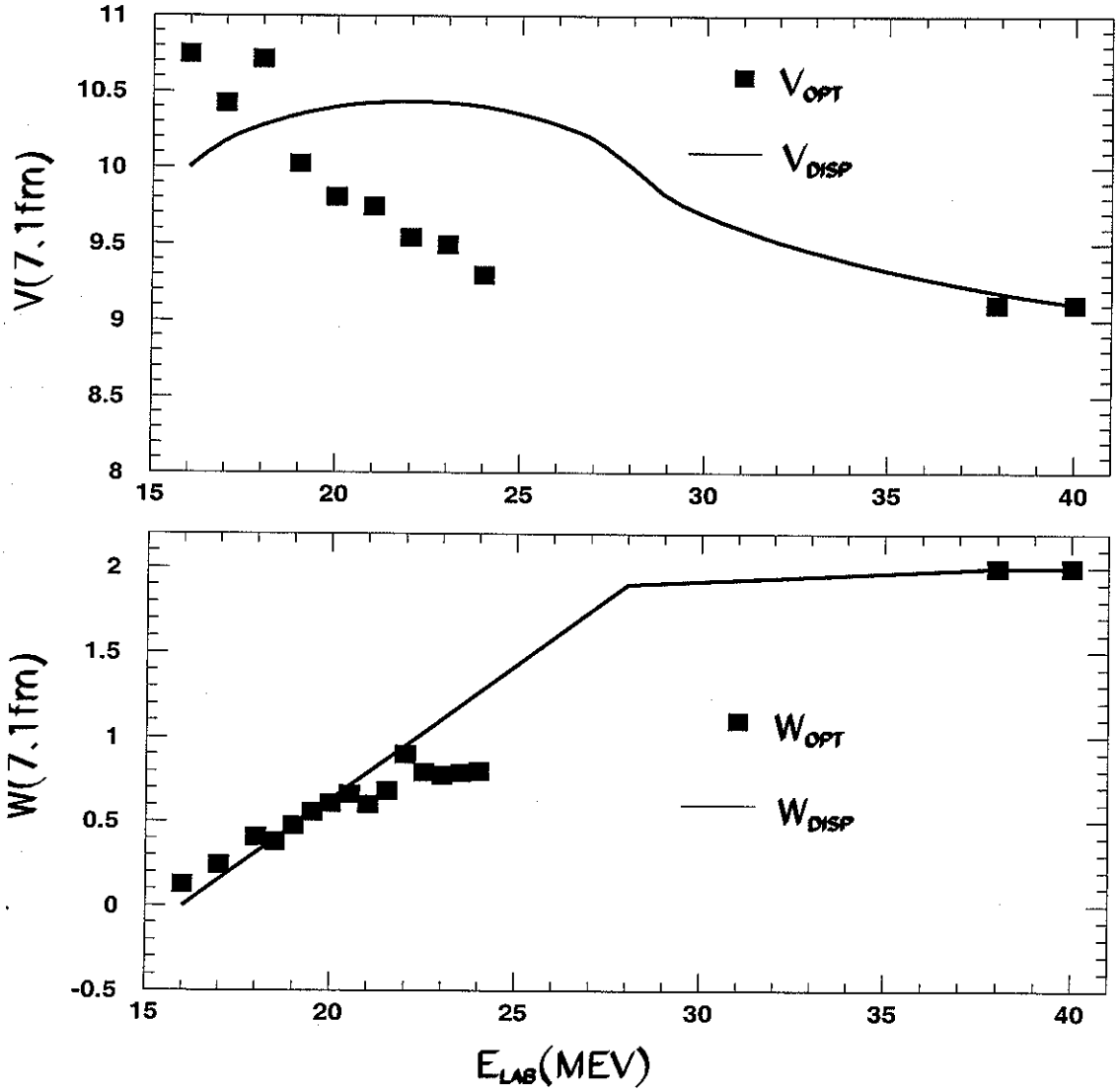
V(7.1fm)
W(7.1fm)
V_{OPT}
V_{DISP}
W_{OPT}
W_{DISP}
E_{LAB}(MEV)

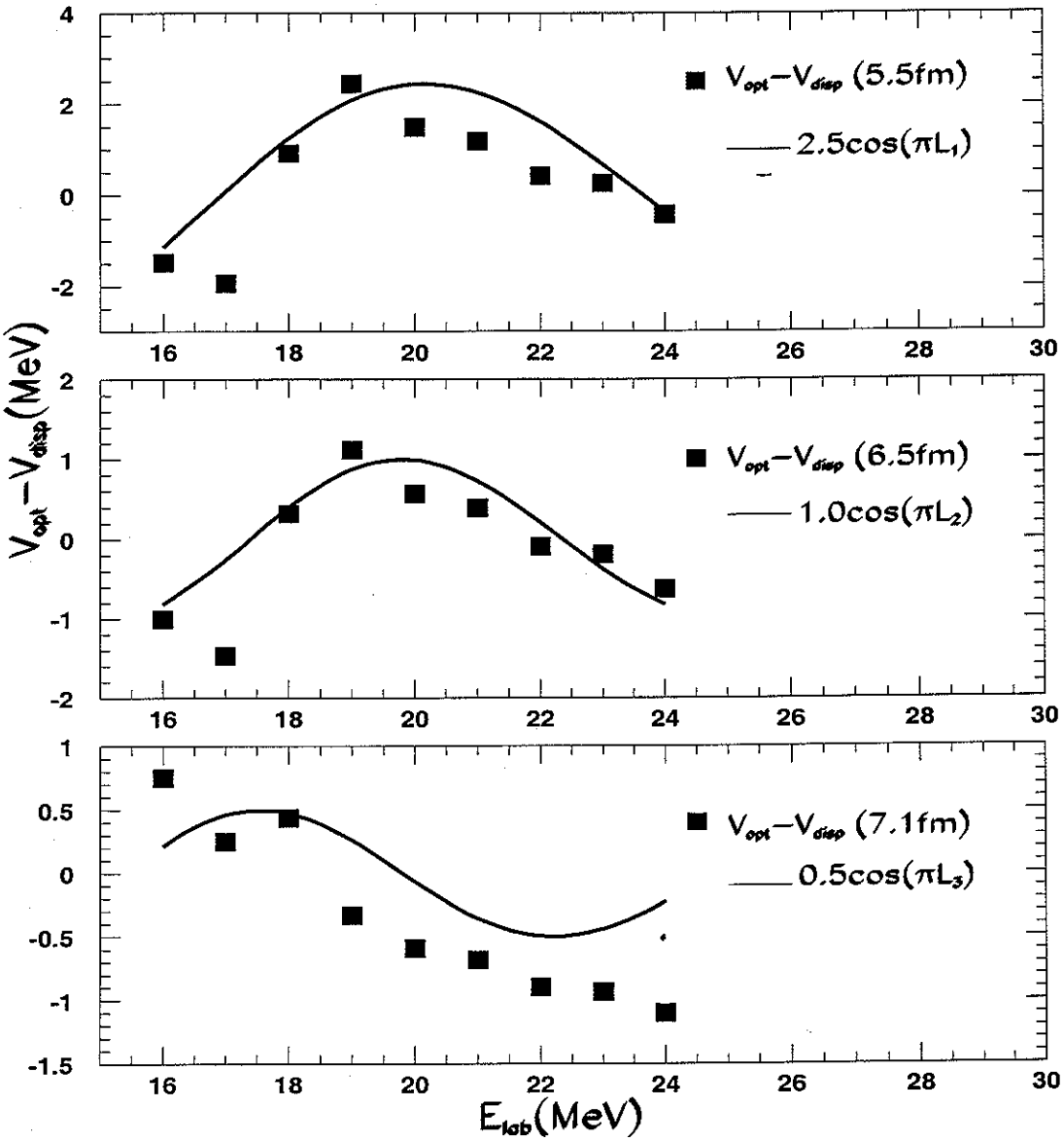
$V_{opt}-V_{disp}$ (5.5fm)
2.5cos(πL₁)
$V_{opt}-V_{disp}$ (6.5fm)
1.0cos(πL₂)
$V_{opt}-V_{disp}$ (7.1fm)
0.5cos(πL₃)
$V_{opt}-V_{disp}$(MeV)
E_{lab}(MeV)